Electronic Supplementary Material (ESI) for Physical Chemistry Chemical Physics.

Electronic Supporting Information for:

Micellization of alkyltrimethylammonium bromide surfactants in choline chloride:glycerol deep eutectic solvent

Adrian Sanchez-Fernandez[a,b], Thomas Arnold[c], Andrew J. Jackson[b,e†], Sian L. Fussell[a], Richard K. Heenan[d], Richard A. Campbell, Karen J. Edler[a]

[a] *Department of Chemistry, University of Bath, Claverton Down, Bath, BA2 7AY, UK.*
[b] *European Spallation Source, Lund, Sweden.*
[c] *Diamond Light Source, Harwell Campus, Didcot, OX11 0DE, UK.*
[d] *ISIS Spallation Neutron Source, Harwell Campus, Didcot OX11 0QX, UK.*
[e] *Department of Physical Chemistry, Lund University, SE-221 00, Lund, Sweden.*
[f] *Institut Laue-Langevin - BP 156, 38.042 Grenoble Cedex 9, France*
[†] Corresponding author: andrew.jackson@esss.se

Surface tension

The diffusion of surfactant to the air liquid interface drives the equilibration of the system. In order to evaluate the validity of our data we have measured changes in the surface tension with the passing of time. The surface tension of pure solvent and different concentrations below the critical micelle concentration (CMC) for C_{12}TAB and C_{16}TAB were measured until the equilibrium was achieved. Fig. S1 shows the evolution of the surface tension with time for those samples.

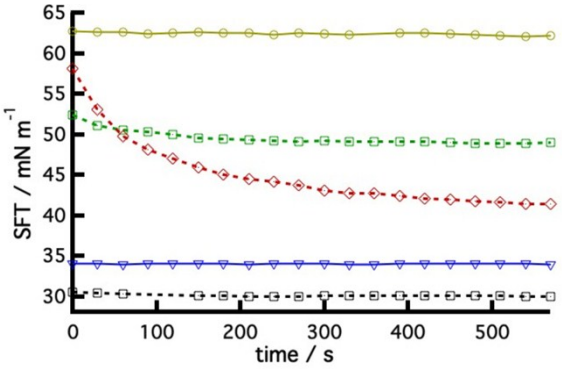

Fig. S1 Contains the evolution of surface tension with time for the (yellow circles) pure solvent and different concentrations of C_{12}TAB and C_{16}TAB: (green squares) 4.2 mM and (blue triangles) 32 mM of C_{12}TAB, and (red rhombus) 0.38 mM and (black squares) 1.0 mM of C_{16}TAB.

Those concentrations close to the CMC have reached the equilibrium state after a few seconds. However, the lowest concentration needed longer to equilibrate. Also, larger surfactant tails needed longer equilibration times. Accounting for this, we have determined the surface tension of the different surfactants in choline chloride:glycerol.

Small-angle neutron scattering model test

Different reciprocal-space models were tested to find the most suitable option to fit the present SANS data. An intermediate concentration of each surfactant was therefore fitted to different models to evaluate the deviations of the fits through the Chi square statistical parameter, which is inversely related to the quality of the fit. A spherical model (Schulz radius distribution), ellipsoidal model, cylindrical model and a core-shell ellipsoidal model (micelle and reverse-micelle cross section) were tested. Fig. S2 includes the best possible fits of each model to data involved C_{16}TAB and Table S1 shows the Chi square parameters of the best fits.

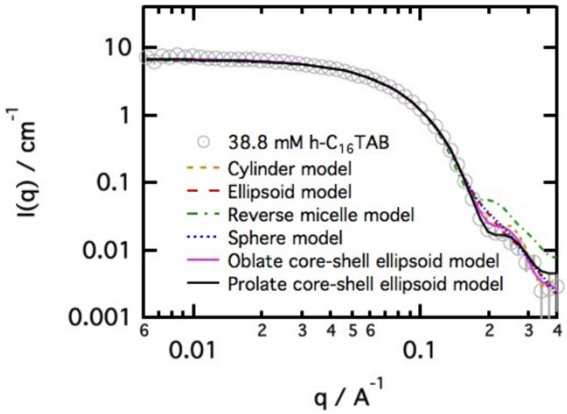

Fig. S2 Different reciprocal-space models tested for 38.8 mM h-C_{16}TAB in d-choline chloride-glycerol. The reverse-micelle ellipsoid model was shown to reduce the core size to a minimum value, ~0, and adjustment of the particle structure by expanding the shell, instead suggesting that a particle with this configuration does not give a physically realistic interpretation of the data.

Model	Chi square/Number of points
Prolate core-shell ellipsoid	1.32
Oblate core-shell ellipsoid	6.45
Polydisperse spheres	11.4
Ellipsoid	11.7

Cylinder	10.8
Reverse core-shell ellipsoid	132

Table S1 Chi square parameters obtained through the fitting using reciprocal-space models shown in Fig. S2.

Subtle differences were found between the three simple models: ellipsoid, sphere and cylinder. These models have provided a similar fit quality. However, due to the apparent size of the aggregate (L/D ratio of ~1.6), the cylinder model was found not to be the best picture of the micelle. Also, the ellipsoid model allows direct comparison our results with previous studies in water.

Co-refinement of all the contrasts allowed to build a more detailed picture of the micelle using a core-shell ellipsoid model. A prolate core-shell ellipsoid model was selected as the best model to fit these data. Since morphology transitions appear to not happen in the present systems, this form factor model was used to fit the data from the whole range of surfactant concentrations. This model was found to provide similar results to the oblate distribution of mass, but considering previous studies in water[1, 2], we have decided to use the prolate distribution in order to directly compare our results.

A rather big deviation to a possible reverse-micelle structure was found when testing the model. The first attempt drove to a physically unrealistic model where the headgroups were occupying a non-existing volume at the centre of the micelle. Therefore this model was rejected.

Samples with high surfactant concentrations were found to contain an intramicellar contribution. We therefore used the model which contains the hard-sphere structure factor combined with the ellipsoidal form factor in order to fit the data, as explained in the main text.

Small-angle neutron scattering results

The size and shape of the micelle core was determined through individual fits of intermediate concentrations of the systems: h-choline chloride:h-glycerol + d-C_n-h-TAB, where the scattering is entirely dominated by the contrasts between the deuterated tails and the solvent. Fig. S3 shows these intermediate concentrations with the best fits for the three surfactants. The results of these fits were subsequently used to fix the size of the micelle core and simultaneously fit all the contrasts.

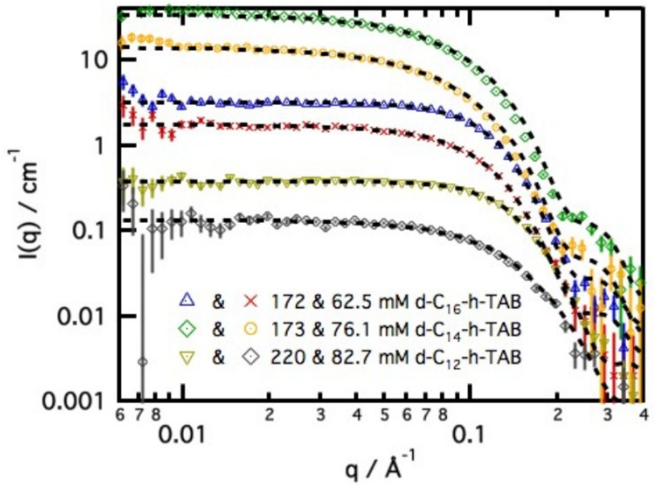

Fig. S3 Intermediate concentrations of the contrast h-choline chloride:h-glycerol + d-C_n-h-TAB (n=12, 14 and 16) with the best fits (black dashed lines).

Data in different isotopic contrasts were measured and simultaneously analysed in order to resolve the micelle structure. Due to the lack of availability of fully deuterated C_{12}TAB (d-C_{12}-d-TAB), three contrasts were used following the same approach. Here we present data and model fits of all the contrasts for each surfactant-deep eutectic solvent system: (Fig. S3 and Table S2) C_{12}TAB, (Fig. S4 and Table S3) C_{14}TAB and (Fig. S5 and Table S4) C_{16}TAB.

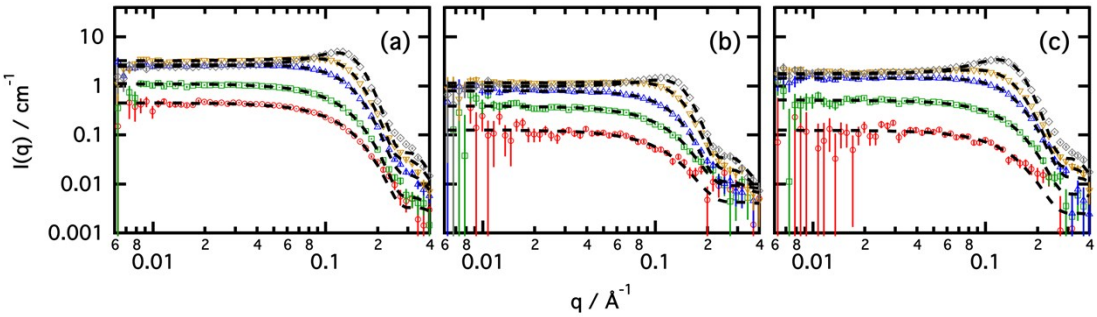

Fig. S4 Isotopic mixtures used to resolve the structure of C_{12}TAB micelles in choline chloride:glycerol: (a) h-C_{12}-h-TAB in d-choline chloride:d-glycerol, (b) h-C_{12}-h-TAB in d-choline chloride:h-glycerol and (c) d-C_{12}-h-TAB in h-choline chloride:h-glycerol.

Conc. / mM	r_{eq} / Å	X_{core}	T_{eq} / Å	X_{shell}	ϕ_{fit}	$\phi_{S(q)}$	Shell SLD / $\times10^{-6}$ Å^2
d-choline chloride:d-glycerol + h-C_{12}-h-TAB							
47.2	14.8±0.3	1.64±0.01	4.4±1.8	1.81±0.49	0.85±0.15	1.8±0.3	5.1±0.8
81.7	14.8±0.3	1.64±0.01	3.8±1.5	1.50±0.42	1.6±0.4	2.1±0.2	4.6±1.1
220	14.8±0.3	1.64±0.01	4.6±0.4	1.13±0.1	5.4±0.4	7.4±0.1	4.2±0.3
455	14.8±0.3	1.64±0.01	4.4±0.2	1.43±0.16	11±1	15±1	3.6±0.2
1019	14.8±0.3	1.64±0.01	4.9±0.1	1.82±0.1	24±1	27±1	4.3±0.1
d-choline chloride:h-glycerol + h-C_{12}-h-TAB							
43.2	14.8±0.3	1.64±0.01	4.4±1.8	1.81±0.49	0.78±0.21	1.8±0.3	1.2±0.4
82.2	14.8±0.3	1.64±0.01	3.8±1.5	1.50±0.42	2±0.7	2.1±0.2	0.6±1.2
190	14.8±0.3	1.64±0.01	4.6±0.4	1.13±0.28	4.5±0.5	7.4±0.1	0.0±0.4
450	14.8±0.3	1.64±0.01	4.4±0.2	1.43±0.16	12±1	15±1	0.1±0.1
997	14.8±0.3	1.64±0.01	4.9±0.1	1.82±0.1	23±1	27±1	0.1±0.2
h-choline chloride:h-glycerol + d-C_{12}-h-TAB							
40.0	14.8±0.3	1.64±0.01	4.4±1.8	1.81±0.49	0.32±0.26	1.8±0.3	0.5±0.3
75.4	14.8±0.3	1.64±0.01	3.8±1.5	1.50±0.42	1.2±0.3	2.1±0.2	0.6±0.1
203	14.8±0.3	1.64±0.01	4.6±0.4	1.13±0.28	4.5±0.3	7.4±0.1	1.1±0.1
360	14.8±0.3	1.64±0.01	4.4±0.2	1.43±0.16	9.4±0.1	15±1	1.0±0.1
813	14.8±0.3	1.64±0.01	4.9±0.1	1.82±0.1	20±1	27±1	2.1±0.1

Table S2 Fitting results of each contrast of C_{12}TAB in choline chloride:glycerol, from Fig. S4.

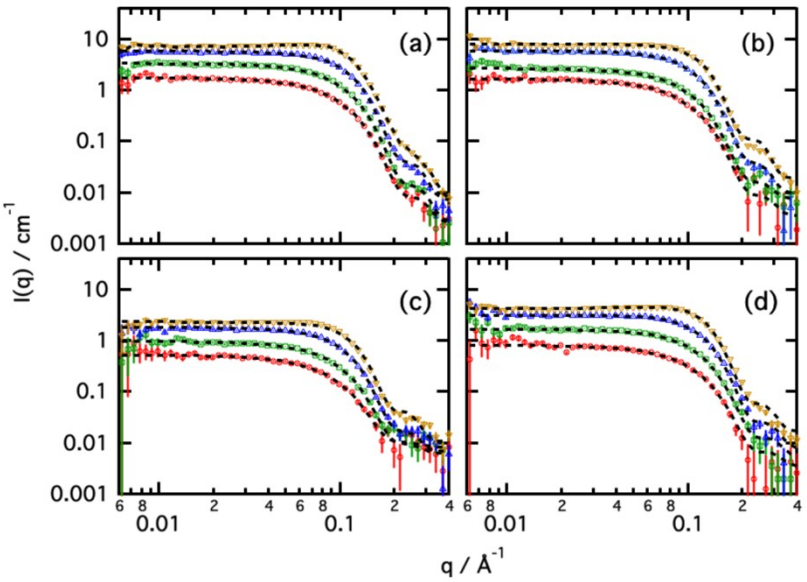

Fig. S5 Isotopic mixtures used to resolve the structure of C_{14}TAB micelles in choline chloride:glycerol: (a) h-C_{14}-h-TAB in d-choline chloride:d-glycerol, (b) d-C_{14}-d-TAB in h-choline chloride:h-glycerol, (c) h-C_{14}-h-TAB in d-choline chloride:h-glycerol and (d) d-C_{14}-h-TAB in h-choline chloride:h-glycerol.

Conc. / mM	r_{eq} / Å	X_{core}	T_{eq} / Å	X_{shell}	$ø_{fit}$	$ø_{S(q)}$	Shell SLD / $\times10^{-6}$ Å^2
d-choline chloride:d-glycerol + h-C_{14}-h-TAB							
42.5	18.9±0.1	1.71±0.04	4.2±2.3	1.11±0.95	1.2±0.2	2.9±0.4	4.5±1.2
87.6	18.9±0.1	1.71±0.04	5.3±1.1	1.25±0.38	2.8±0.3	5.2±0.3	4.6±0.5
191	18.9±0.1	1.71±0.04	4.4±0.2	1.56±0.09	5.5±0.2	11±1	4.1±0.2
429	18.9±0.1	1.71±0.04	4.7±0.1	1.62±0.10	4.7±0.1	18±1	3.3±0.1
h-choline chloride:h-glycerol + d-C_{14}-d-TAB							
37.9	18.9±0.1	1.71±0.04	4.2±2.3	1.11±0.95	1±0.2	2.9±0.4	2.9±1.6
67.9	18.9±0.1	1.71±0.04	5.3±1.1	1.25±0.38	1.9±0.2	5.2±0.3	3.1±0.7
173	18.9±0.1	1.71±0.04	4.4±0.2	1.56±0.09	5.7±0.3	11±1	3.2±0.3
363	18.9±0.1	1.71±0.04	4.7±0.1	1.62±0.10	11±1	18±1	4.8±0.1
d-choline chloride:h-glycerol + h-C_{14}-h-TAB							
44.7	18.9±0.1	1.71±0.04	4.2±2.3	1.11±0.95	1.2±0.1	2.9±0.4	0.1±0.2
80.0	18.9±0.1	1.71±0.04	5.3±1.1	1.25±0.38	3.1±0.1	5.2±0.4	0.8±0.6
193	18.9±0.1	1.71±0.04	4.4±0.2	1.56±0.09	6.7±0.1	11±1	0.5±0.3
422.66	18.9±0.1	1.71±0.04	4.7±0.2	1.62±0.10	13±1	18±1	0.2±0.1
h-choline chloride:h-glycerol + d-C_{14}-h-TAB							
36.14	18.9±0.1	1.71±0.04	4.2±2.3	1.11±0.95	0.79±0.16	2.9±0.4	0.5±0.3
76.07	18.9±0.1	1.71±0.04	5.3±1.1	1.25±0.38	2.2±0.2	5.2±0.3	0.6±0.1
173	18.9±0.1	1.71±0.04	4.4±0.2	1.56±0.09	5.2±0.2	11±1	1.3±0.1
347	18.9±0.1	1.71±0.04	4.7±0.1	1.62±0.10	11±1	18±1	1.6±0.1

Table S3 Fitting results of each contrast of C_{14}TAB in choline chloride:glycerol, from Fig. S5.

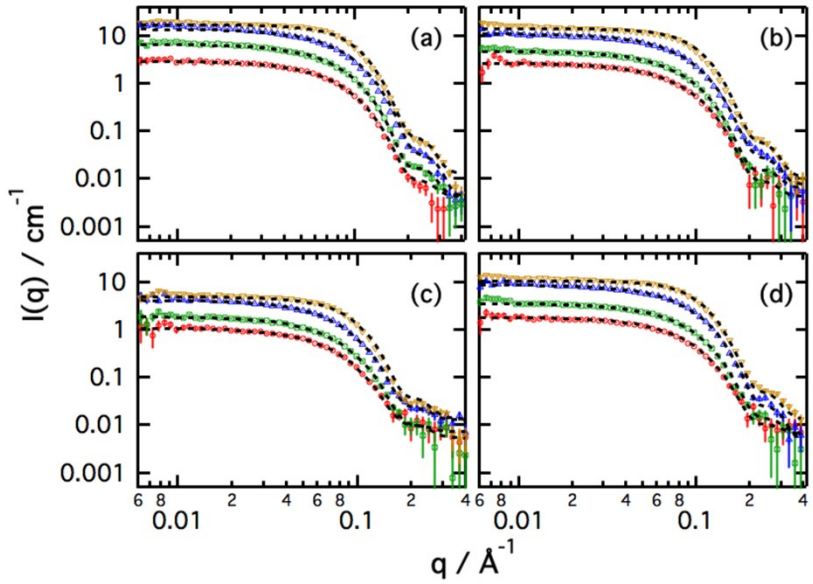

Fig. S6 Isotopic mixtures used to resolve the structure of C_{16}TAB micelles in choline chloride:glycerol: (a) h-C_{16}-h-TAB in d-choline chloride:d-glycerol, (b) d-C_{16}-d-TAB in h-choline chloride:h-glycerol, (c) h-C_{16}-h-TAB in d-choline chloride:h-glycerol and (d) d-C_{16}-h-TAB in h-choline chloride:h-glycerol.

Conc. / mM	r_{eq} / Å	X_{core}	T_{eq} / Å	X_{shell}	ϕ_{fit} / ×10^{-2}	$\phi_{S(q)}$ / ×10^{-2}	Shell SLD / ×10^{-6} Å^2
d-choline chloride:d-glycerol + h-C_{16}-h-TAB							
38.8	19.6±0.1	1.82±0.05	5.6±1.5	1.84±0.20	1.2±0.2	0±0.2	4.0±0.6
75.0	19.6±0.1	1.82±0.05	5.4±0.5	1.85±0.12	2.7±0.2	0±0.1	4.0±0.3
182	19.6±0.1	1.82±0.05	5.7±0.5	1.72±0.12	4.2±0.1	0.7±0.1	4.8±0.2
378	19.6±0.1	1.82±0.05	6.1±0.2	1.74±0.03	11±1	8.9±0.1	3.6±0.1
h-choline chloride:h-glycerol + d-C_{16}-d-TAB							
35.2	19.6±0.1	1.82±0.05	5.6±1.5	1.84±0.20	1.2±0.2	0±0.2	2.4±0.5
65.1	19.6±0.1	1.82±0.05	5.4±0.5	1.85±0.12	2.2±0.2	0±0.1	2.3±0.3
160	19.6±0.1	1.82±0.05	5.7±0.5	1.72±0.12	5.9±0.1	0.7±0.1	2.4±0.2
340	19.6±0.1	1.82±0.05	6.1±0.2	1.74±0.03	12±1	8.9±0.1	2.6±0.1
d-choline chloride:h-glycerol + h-C_{16}-h-TAB							
39.3	19.6±0.1	1.82±0.05	5.6±1.5	1.84±0.20	1.5±0.1	0±0.22	0.4±0.2
70.7	19.6±0.1	1.82±0.05	5.4±0.5	1.85±0.12	2.7±0.2	0±0.1	0.2±0.1
174	19.6±0.1	1.82±0.05	5.7±0.5	1.72±0.12	5.5±0.1	0.7±0.1	0.8±0.1
359	19.6±0.1	1.82±0.05	6.1±0.2	1.74±0.03	12±1	8.9±0.1	0.3±0.1
h-choline chloride:h-glycerol + d-C_{16}-h-TAB							
31.9	19.6±0.1	1.82±0.05	5.6±1.5	1.84±0.20	1.1±0.1	0±0.2	1.3±0.2
62.5	19.6±0.1	1.82±0.05	5.4±0.5	1.85±0.12	2.2±0.2	0±0.1	1.6±0.2
172	19.6±0.1	1.82±0.05	5.7±0.5	1.72±0.12	5.7±0.1	0.7±0.1	1.2±0.2
333	19.6±0.1	1.82±0.05	6.1±0.2	1.74±0.03	10±1	8.9±0.1	1.8±0.1

Table S4 Fitting results of each contrast of C_{16}TAB in choline chloride:glycerol, from Fig. S6.

References

1. S. S. Berr, *J. Phys. Chem.*, 1987, **91**, 4760-4765.
2. S. S. Berr, E. Caponetti, J. S. Johnson, R. R. M. Jones and L. J. Magid, *J. Phys. Chem.*, 1986, **90**, 5766-5770.